Inorg. Chem. **2005**, *44*, 8610–8616

Formation and Characterization of Thorium Methylidene CH_2═ThHX Complexes

Jonathan T. Lyon and Lester Andrews*

Department of Chemistry, University of Virginia, P.O. Box 400319, Charlottesville, Virginia 22901-4319

Received July 11, 2005

Laser-ablated thorium atoms react with methyl fluoride to give the CH_2═ThHF molecule as the major product observed and trapped in solid argon. Infrared spectroscopy, isotopic substitution, and density functional theoretical frequency calculations confirm the identification of this methylidene complex. The four strongest computed absorptions (Th–H stretch, Th═C stretch, CH_2 wag, and Th–F stretch) are the four vibrational modes observed. The CH_2═ThHCl and CH_2═ThHBr species formed from methyl chloride and methyl bromide exhibit the first three of these modes in the infrared spectra. The computed structures (B3LYP and CCSD) show considerable agostic interaction, similar to that observed for the Group 4 CH_2═MHX (M = Ti, Zr, Hf) methylidene complexes, and the agostic angle and C═Th bond length decrease slightly in the CH_2═ThHX series (X = F, Cl, Br).

Introduction

Investigations of Group 4 early transition-metal atom reactions with methyl halides in our group over the past year have provided spectroscopic and computational evidence for the simple methylidene complexes CH_2═MHX that are formed by α−H transfer within the initial CH_3−MX insertion product.[1−4] Two interesting trends have been noted: First, the agostic distortion (as measured by the calculated H−C−M angle and C−H bond length) decreases Ti to Zr to Hf as the C═M bond length increases, and second the agostic distortion increases F to Cl to Br as the C═Ti bond length decreases. The corresponding reactions with methane give lower product yields, but form the analogous simple methylidene complexes, which show agostic distortion in structures from B3LYP calculations with large basis sets and, in the matrix, infrared spectra of different CHD═MHD structural isomers.[5−8] Again, the agostic distortion decreases Ti to Zr to Hf as the C═M bond length increases. We have subsequently performed more rigorous CCSD calculations for the Group 4 CH_2═MH_2 molecules and find slightly more agostic distortion with the same trend.[9]

In many respects the chemistry of thorium parallels that of the Group 4 metals.[10,11] Similar metallocene complexes have been formed with Zr and Th.[12−14] In matrix isolation experiments, similar hydrides, particularly MH_4, and oxides have been produced.[15−18] Along this line, a large number of alkylidene complexes with Group 4 metals have been investigated for applications as catalysts in alkene metathesis and alkane activation reactions,[19,20] but the analogous actinide alkylidene complexes have not been prepared.[20,21] Related

* To whom correspondence should be addressed. E-mail: lsa@virginia.edu.

(1) Cho, H.-G.; Andrews, L. *J. Phys. Chem. A* **2004**, *108*, 6294 (Ti + CH_3F).
(2) Cho, H.-G.; Andrews, L. *J. Am. Chem. Soc*. **2004**, *126*, 10485 (Zr + CH_3F).
(3) Cho, H.-G.; Andrews, L. *Organometallics* **2004**, *23*, 4357 (Hf + CH_3F).
(4) Cho, H.-G.; Andrews, L. *Inorg. Chem*. **2005**, *44*, 979 (Ti + CH_3X).
(5) Andrews, L.; Cho, H.-G.; Wang, X. *Angew. Chem., Int. Ed*. **2005**, *44*, 113 (Zr + CH_4).
(6) Cho, H.-G.; Wang, X.; Andrews, L. *J. Am. Chem. Soc*. **2005**, *127*, 465 (Zr + CH_4).
(7) Cho, H.-G.; Wang, X.; Andrews, L. *Organometallics* **2005**, *24*, 2854 (Hf + CH_4).
(8) Andrews, L.; Cho, H.-G.; Wang, X. *Inorg. Chem.* **2005**, *44*, 4834 (Ti + CH_4).
(9) Cho, H.-G.; Andrews, L. Unpublished calculations.
(10) Cotton, F. A.; Wilkinson, G.; Murillo, C. A.; Bochmann, M. *Advanced Inorganic Chemistry*, 6th ed.; Wiley: New York, 1999.
(11) Pyykko, P. *Chem. Rev.* **1988**, *88*, 563.
(12) Hlatky, G. G.; Eckman, R. R.; Turner, H. W. *Organometallics* **1992**, *11*, 1413.
(13) Yang, X.; King, W. A.; Sabat, M.; Marks, T. J. *Organometallics* **1993**, *12*, 4254.
(14) Chen, E. Y.-X.; Marks, T. J. *Chem. Rev.* **2000**, *100*, 1391.
(15) Chertihin, G. V.; Andrews, L. *J. Phys. Chem*. **1995**, *99*, 15004 (Zr + H_2).
(16) Souter, P. F.; Kushto, G. P.; Andrews, L.; Neurock, M. *J. Phys. Chem. A* **1997**, *101*, 1287 (Th + H_2).
(17) Chertihin, G. V.; Andrews, L. *J. Phys. Chem*. **1995**, *99*, 6356.
(18) Gabelnick, S. D.; Reedy, G. T.; Chasanov, M. G. *J. Chem. Phys*. **1974**, *60*, 1167.
(19) Crabtree, R. H. *Chem. Rev*. **1985**, *85*, 245.
(20) Schrock, R. R. *Chem. Rev*. **2002**, *102*, 145.

10.1021/ic051153w CCC: $30.25
Published on Web 10/19/2005

uranium−carbon multiple bonded complexes and surface-stabilized alkylidene species with actinide metals have been studied.[22,23] Hence, it would be of interest to synthesize the simple thorium methylidene complexes for comparison to Group 4 analogues. In this regard, we have formed CH_2═ThH_2 through the Th and CH_4 reaction, and our B3LYP and CCSD calculations find the agostic distortion to be nearly the same as that computed for CH_2═HfH_2.[7,9,24] We wish to report here the halogen-substituted thorium methylidene complexes, CH_2═ThHX, prepared from methyl fluoride, chloride, and bromide, which exhibit similar agostic distortion.

Experimental and Theoretical Methods

Laser-ablated Th atoms were reacted with CH_3X molecules (Matheson) and isotopic modifications at 0.5% concentrations in excess argon during condensation onto an 8 K cesium iodide window, as described previously.[1,4,16,25,26] Infrared spectra were recorded on a Nicolet 550 spectrometer after sample deposition, after annealing, and after irradiation by a common mercury-arc street lamp. Theoretically, the structures and vibrational frequencies of the CH_3−ThX and CH_2═ThHX molecules were calculated using the Gaussian 98 methods employed for the Group 4 complexes.[1−4,27] Here, the B3LYP density functional was used with the large 6-311++G(3df,3pd) basis set, and relativistic effects were included in the SDD pseudopotential for thorium (30 valence electrons).[28,29] The vibrational frequencies were computed analytically. For comparison, more rigorous coupled-cluster, with single and double substitutions (CCSD), structure calculations were done using the NWChem program.[30]

Results and Discussion

Reactions of laser-ablated Th atoms with methyl halide precursors in excess argon during condensation will be described in turn.

CH_3F. The Th and CH_3F reaction in excess argon gives four pairs of new infrared absorptions at 1392.2 and 1380.5 cm^{-1}, 674.1 and 670.4 cm^{-1}, 634.0 and 626.4 cm^{-1}, and 524.6 and 518.6 cm^{-1} for one major new product molecule. The infrared spectrum is shown in Figure 1, where the above absorptions are labeled **1** and **2**. Irradiation with near-ultraviolet light (λ > 290 nm Pyrex filter) increased the **1** band in each pair by 10% and doubled the **2** band, and exposure to the full mercury arc (λ > 220 nm, unfiltered) increased the **1** bands by 20% and the **2** bands by 10%. Next, annealing at 30 K decreased **1** and increased **2**; then full-arc irradiation reversed these changes, and a final 35 K annealing substantially decreased **1** and increased **2**. It appears that ultraviolet irradiation and annealing affect reversible changes in the trapping environment of the major reaction product.

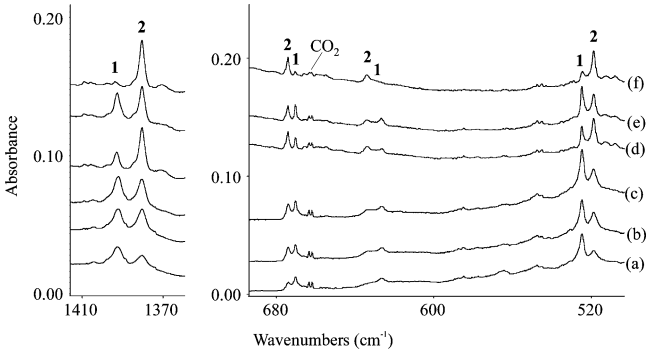

Figure 1. Infrared spectra in the 1410−1370 and 680−520 cm^{-1} regions for laser-ablated Th atoms co-deposited with CH_3F in excess Ar at 8 K: (a) Th + 0.5% CH_3F in Ar co-deposited for 1 h, (b) after photolysis with a Pyrex filter, (c) after photolysis without a filter, (d) after annealing at 30 K, (e) after photolysis without a filter, and (f) after annealing at 35 K.

Next, methyl fluoride isotopic modifications were used to characterize the product absorptions. Methyl fluoride-^{13}C had no significant effect on the upper bands, but shifted the lower bands as listed in Table 1. The band pairs exhibited the same reversal in band intensities on irradiation and annealing as observed with CH_3F. Deuterated methyl fluoride displaced the band pairs to 995.2 cm^{-1} and under precursor, 619.3 and 615.0 cm^{-1}, 521.3 and 513.3 cm^{-1}, and weak bands at 501.2 and 494.2 cm^{-1}. Figure 2 compares the spectra in the lower-wavenumber region for three isotopic precursors for the spectrum after irradiation, which gives the strongest product absorptions.

The four pairs of new infrared absorptions increase and decrease together upon sample irradiation and annealing, and they can be assigned to the same reaction product trapped in two different argon matrix-packing configurations. These absorptions closely follow those observed for the CH_2═ZrHF and CH_2═HfHF molecules,[2,3] which are compared in Table 2. The 1392.2 cm^{-1} band shifts to 995.2 cm^{-1} with CD_3F,

(21) Pool, J. A.; Scott, B. L.; Kiplinger, J. L. *J. Am. Chem. Soc.* **2005**, *127*, 1338.
(22) For example, see: Cramer, R. E.; Maynard, R. B.; Paw, J. C.; Gilje, J. W. *J. Am. Chem. Soc.* **1981**, *103*, 3589.
(23) He, M.-Y.; Xiong, G.; Toscano, P. J.; Burwell, R. L., Jr.; Marks, T. J. *J. Am. Chem. Soc.* **1985**, *107*, 641.
(24) Andrews, L.; Cho, H.-G. *J. Phys. Chem. A* **2005**, *109*, 6796 (Th + CH_4).
(25) Liang, B.; Andrews, L.; Li, J.; Bursten, B. E. *J. Am. Chem. Soc.* **2002**, *124*, 6723.
(26) Andrews, L. *Chem. Soc. Rev.* **2004**, *33*, 123 and references therein.
(27) Frisch, M. J.; Trucks, G. W.; Schlegel, H. B.; Scuseria, G. E.; Robb, M. A.; Cheeseman, J. R.; Zakrzewski, V. G.; Montgomery, J. A., Jr.; Stratmann, R. E.; Burant, J. C.; Dapprich, S.; Millam, J. M.; Daniels, A. D.; Kudin, K. N.; Strain, M. C.; Farkas, O.; Tomasi, J.; Barone, V.; Cossi, M.; Cammi, R.; Mennucci, B.; Pomelli, C.; Adamo, C.; Clifford, S.; Ochterski, J.; Petersson, G. A.; Ayala, P. Y.; Cui, Q.; Morokuma, K.; Rega, N.; Salvador, P.; Dannenberg, J. J.; Malick, D. K.; Rabuck, A. D.; Raghavachari, K.; Foresman, J. B.; Cioslowski, J.; Ortiz, J. V.; Baboul, A. G.; Stefanov, B. B.; Liu, G.; Liashenko, A.; Piskorz, P.; Komaromi, I.; Gomperts, R.; Martin, R. L.; Fox, D. J.; Keith, T.; Al-Laham, M. A.; Peng, C. Y.; Nanayakkara, A.; Challacombe, M.; Gill, P. M. W.; Johnson, B.; Chen, W.; Wong, M. W.; Andres, J. L.; Gonzalez, C.; Head-Gordon, M.; Replogle, E. S.; Pople, J. A. *Gaussian 98*, revision A.11.4; Gaussian, Inc.: Pittsburgh, PA, 2002 and references therein.
(28) Frisch, M. J.; Pople, J. A.; Binkley, J. S. *J. Chem. Phys.* **1984**, *80*, 3265.
(29) Küchle, W.; Dolg, M.; Stoll, H.; Preuss, H. *J. Chem. Phys.* **1994**, *100*, 7535.
(30) Aprà, E.; Windus, T. L.; Straatsma, T. P.; Bylaska, E. J.; de Jong, W.; Hirata, S.; Valiev, M.; Hackler, M.; Pollack, L.; Kowalski, K.; Harrison, R.; Dupuis, M.; Smith, D. M. A.; Nieplocha, J.; Tipparaju V.; Krishnan, M.; Auer, A. A.; Brown, E.; Cisneros, G.; Fann, G.; Früchtl, H.; Garza, J.; Hirao, K.; Kendall, R.; Nichols, J.; Tsemekhman, K.; Wolinski, K.; Anchell, J.; Bernholdt, D.; Borowski, P.; Clark, T.; Clerc, D.; Dachsel, H.; Deegan, M.; Dyall, K.; Elwood, D.; Glendening, E.; Gutowski, M.; Hess, A.; Jaffe, J.; Johnson, B.; Ju, J.; Kobayashi, R.; Kutteh, R.; Lin, Z.; Littlefield, R.; Long, X.; Meng, B.; Nakajima, T.; Niu, S.; Rosing, M.; Sandrone, G.; Stave, M.; Taylor, H.; Thomas, G.; van Lenthe, J.; Wong, A.; Zhang, Z. *NWChem, A Computational Chemistry Package for Parallel Computers*, version 4.6; Pacific Northwest National Laboratory: Richland, WA, 2004.

Table 1. Observed and Calculated Fundamental Frequencies of CH_2═ThHF in the Singlet Ground Electronic State[a]

approximate mode description	CH_2═ThHF		$^{13}CH_2$═ThHF		CD_2═ThDF	
	obsd[b]	calcd (int)	obsd[b]	calcd (int)	obsd[b]	calcd (int)
CH stretch		3142.5 (4)		3132.2 (4)		2321.1 (1)
CH stretch		2852.9 (17)		2846.1 (18)		2079.0 (5)
Th−H stretch	1392.2, **1380.5**	1421.7 (463)	1392.1, **1380.5**	1421.6 (462)	995.2, −[c]	1021.8 (95)
CH_2 bend		1341.5 (20)		1334.9 (22)		1004.4 (156)
Th═C stretch	**674.1**, 670.4	677.2 (124)	**653.4**, 650.2	657.4 (117)	**619.3**, 615.0	617.9 (93)
CH_2 wag	**634.0**, 626.4	646.4 (158)	**629.1**, 621.6	640.9 (53)	**501.2**, 494.2	505.0 (109)
Th−F stretch	524.6, **518.6**	539.1 (204)	524.3, **518.3**	538.8 (205)	521.3, **513.3**	535.2 (179)
CThH bend		475.7 (48)		473.2 (49)		360.7 (23)
CH_2 twist		400.2 (29)		399.0 (27)		290.8 (26)
CH_2 rock		313.8 (70)		313.6 (70)		224.7 (39)
HCThH deformation		271.9 (46)		271.9 (47)		199.2 (18)
CThF bend		119.7 (19)		118.0 (18)		111.0 (16)

[a] Frequencies and intensities are in cm^{-1} and km/mol, respectively. Intensities are all calculated values using at B3LYP/6-311++G(3df,3pd)/SDD. [b] Absorption **2** in each observed pair, which increases on photolysis and annealing, is in bold type. Absorption **1** in each observed pair, which increases less on photolysis and decreases on annealing, is in regular type. [c] Masked by CD_3F precursor.

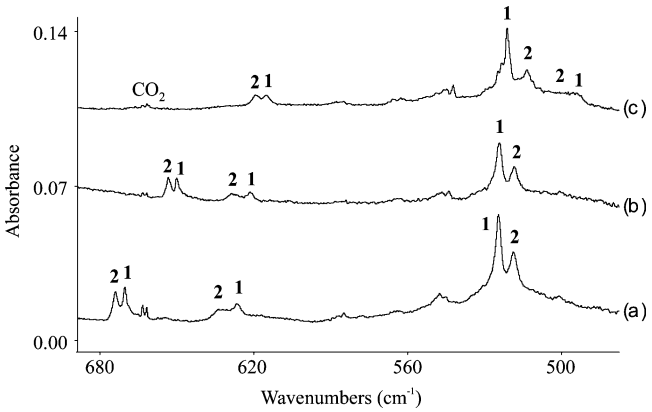

Figure 2. Infrared spectra in the 680−490 cm^{-1} region for laser-ablated Th atoms co-deposited with argon diluted 0.5% samples of (a) CH_3F, (b) $^{13}CH_3F$, and (c) CD_3F. Spectra were recorded after full-arc irradiation.

Table 2. Comparison of Frequencies Observed and Parameters Calculated for Singlet CH_2═MHF Methylidene Complexes in Solid Argon[a]

mode	Ti	Zr	Hf	Th
M−H stretch	1603	1538	1627	1380
M═C stretch	758	740	755	674
CH_2 wag	653	669	646	634
M−F stretch	699	634	634	518
C−M−H bend		559		
C−M bond length (Å)	1.812	1.966	1.979	2.129
H′−C bond length (Å)	1.117	1.118	1.114	1.115
H′−C−M angle (deg)	94.0	95.8	99.2	94.7
q(M)[b]	0.88	1.33	1.21	1.88

[a] Calculated here at the B3LYP/6-311++G(3df,3pd)/SDD level. [b] Mulliken charge.

and the H/D ratio, 1.399, is appropriate for a Th−H(D) vibration, and this frequency is on the lower edge of the Th−H stretching region.[16] The 674.1 cm^{-1} absorption shifts 20.7 cm^{-1} to 653.4 cm^{-1} with $^{13}CH_3F$, and a pure diatomic C−Th harmonic oscillator would shift 25.0 cm^{-1}. This is the region expected for a C═Th double bond stretching mode.[31] Finally, the 518.6 cm^{-1} band shifts only 0.3 cm^{-1} to 518.3 cm^{-1}, and the strong ThF_4 fundamental is at 520 cm^{-1},[32] so our 518.6 cm^{-1} band is probably caused by a Th−F stretching mode. Thus, the IR absorptions describe the actinide methylidene complex CH_2═ThHF.

Density functional theory calculations are helpful for Th + CH_3F reaction product identification following recent work with Ti, Zr, and Hf.[1−3] Our B3LYP calculation found the antisymmetric Th−H stretching mode for singlet state ThH_4 to be only 5 cm^{-1} higher than that observed in solid argon,[16] which is a very good fit for this diagnostic mode. The first product CH_3−ThF triplet ground-state molecule (C−Th, 2.422 Å; Th−F, 2.093 Å), analogous to CH_3−ZrF, has a strong M−F stretching mode, computed at 548 cm^{-1} (98 km/mol) and a C−H deformation mode at 1156 cm^{-1} (36 km/mol), but this molecule is 5 kcal/mol higher in energy than the more stable α-H transfer product CH_2═ThHF in the singlet ground state, which is in contrast to the Hf case, where the two products are isoergic, and the Zr case, where the CH_3−ZrF insertion product is more stable than CH_2═ZrHF by 5 kcal/mol.[2,3] The calculated vibrational frequencies for the singlet ground-state trans-agostic CH_2═ThHF molecule are listed in Table 1, and the structure is illustrated in Figure 3. The agostic H′−C−Th angle is 94.7°. Finally, we calculated the triplet CH_2−ThHF complex, and found it to be almost planar with a longer C−Th bond (2.420 Å), almost equal C−H bond lengths (1.096, 1.093 Å), and 22 kcal/mol higher energy and to have no agostic distortion.

For comparison, the MP2 electronic-structure method was employed with the same large basis set, and the structure is similar to that in Figure 3. The agostic H′−C−Th angle is 88.5°, and other angles and bond lengths follow: H−C−Th, 158.5°; H−C−H, 111.0°; C−Th−H, 98.4°; C−Th−F, 107.7°; H−Th−F, 109.8°; C−H′, 1.119 Å; C−H, 1.085 Å; C═Th, 2.127 Å; Th−H, 2.078 Å; Th−F, 2.111 Å. Finally, a CCSD calculation was performed using NWChem,[30] the 6-311++G(2d,2p) basis set, and the SDD pseudopotential,[28,29] and the structure, shown in Figure 4, is comparable to the DFT structure in Figure 3. This agreement substantiates the use of less time-consuming B3LYP/DFT methods for the calculation of structure and related vibrational frequencies for the thorium methylidene species.

(31) Zhou, M.; Andrews, L.; Li, J.; Bursten, B. E. *J. Am. Chem. Soc.* **1999**, *121*, 12188.

(32) Konings, R. J. M. *J. Chem. Phys.* **1996**, *105*, 9379.

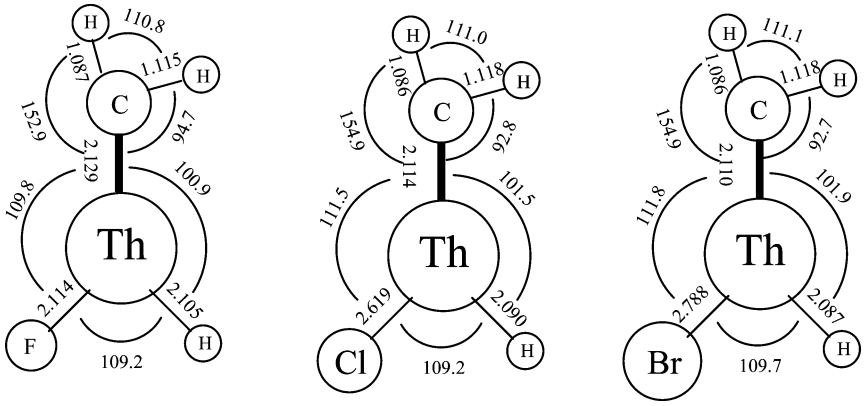

Figure 3. Optimized molecular structures (B3LYP/6-311++G(3df,3pd)/SDD) for CH_2═ThHX (X = F, Cl, Br). Bond lengths are in angstroms and angles are in degrees.

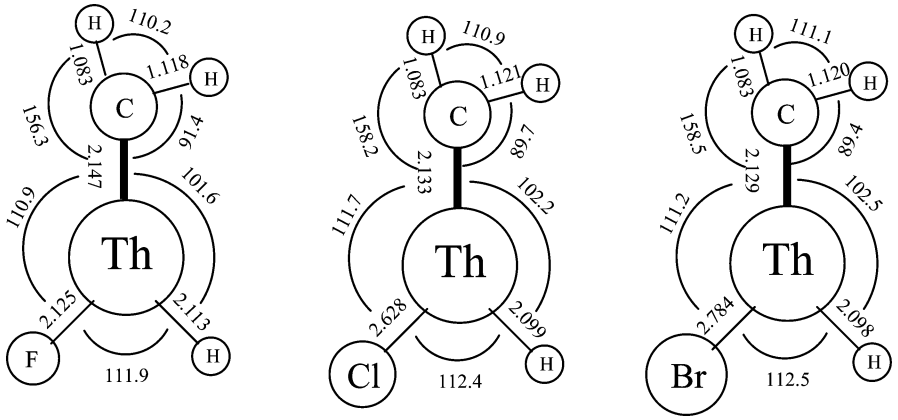

Figure 4. Optimized molecular structures (CCSD/6-311++G(2d,2p)/SDD, 6-311G(d,p) basis for Br) for CH_2═ThHX (X = F, Cl, Br). Bond lengths are in angstroms and angles are in degrees.

We attempted to calculate the cis-agostic isomer CH_2═ThFH, but the calculation converged to the trans-agostic structure using B3LYP. Next, we exchanged C−H bonds and did a fixed-point cis-agostic calculation: this structure is 4 kcal/mol higher in energy than the trans-agostic structure, and all frequencies are real and close to the trans-agostic values (between +7 and −29 cm^{-1}). In fact, we considered these two isomers as a possible explanation of the two IR bands observed for each fundamental frequency, but two of the four frequencies do not fit. We believe it unlikely that argon matrix interaction could prevent CH_2 deformation and cis → trans relaxation in the matrix cage, and thus we expect that the higher energy cis-agostic isomer cannot be trapped in the matrix. Thus, we believe the weaker **1** bands are the result of a less-stable more-repulsive argon matrix trapping site that can be created by UV irradiation and that is relaxed upon annealing the matrix. Similar, but less pronounced effects, are observed for the CH_3Cl and CH_3Br products described next. It must be noted that CH_2═ThHF has a large computed dipole moment (5.07 D) and some matrix interaction is expected for this molecule.

The vibrational frequencies computed for CH_2═ThHF are related to frequencies calculated for the analogous transition-metal methylidenes CH_2═ZrHF and CH_2═HfHF. Note that the Hf−H stretching frequency (1627.3 cm^{-1}) is higher than the Zr−H stretching frequency (1537.8 cm^{-1}) because of relativistic effects, but the Th−H stretching mode (1380.5 cm^{-1}) is lower because of shell expansion.[11] Our B3LYP calculation predicted the Th−H stretching mode at 1421.7 cm^{-1}, which is 3.0% higher than the major 1380.5 cm^{-1} absorption, and the 0.1 cm^{-1} ^{13}C shift is in accord with the experiment. This is the range of quantitative fit for B3LYP computed frequencies.[33] In addition, our calculation predicts that the stronger C−H stretching mode might be observable (4% of Th−H mode intensity) in the region below the very strong 2863 cm^{-1} CH_3F absorption, but no product is observed in this region where the signal-to-noise ratio is not as good as that found at 1400 cm^{-1}.[34] Next, the mostly C−Th stretching mode is calculated at 677.2 cm^{-1} with 19.8 cm^{-1} ^{13}C and 59.3 cm^{-1} D isotopic frequency shifts, which are very close to the observed 674.1 cm^{-1} band, and 20.7, and 54.8 cm^{-1} frequency shifts. Note that the harmonic calculation predicts slightly less carbon and more hydrogen character in this normal mode. The CH_2 wag is predicted at 646.4 cm^{-1} with 5.5 cm^{-1} ^{13}C and 141.4 cm^{-1} D isotopic frequency shifts and observed at 634.0 cm^{-1} with 4.9 and 132.8 cm^{-1} isotopic frequency shifts. Finally, the mostly Th−F stretching mode

(33) Scott, A. P.; Radom, L. *J. Phys. Chem.* **1996**, *100*, 16502.

(34) The only simple CH_2═M species for which C−H stretching frequencies have been observed is CH_2═$Re(O)_2OH$, which is prepared by photolysis of CH_3ReO_3, see: Morris, L. J.; Downs, A. J.; Greene, T. M.; McGrady, G. S.; Herrmann, W. A.; Sirsch, P.; Scherer, W.; Gropen, O. *Organometallics* **2001**, *20*, 2344. It should be noted that we are able to react a very small amount (<1%) of the incident precursor in these laser-ablation metal-source experiments.

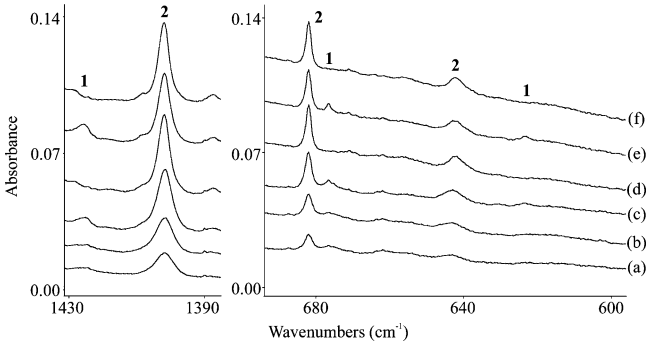

Figure 5. Infrared Spectra in the 1430−1390 and 690−600 cm^{-1} regions for laser-ablated Th atoms co-deposited with CH_3Cl in excess Ar at 8 K: (a) Th + 0.5% CH_3Cl in Ar co-deposited for 1 h, (b) after photolysis with a Pyrex filter, (c) after photolysis without a filter, (d) after annealing at 30 K, (e) after photolysis without a filter, and (f) after annealing at 35 K.

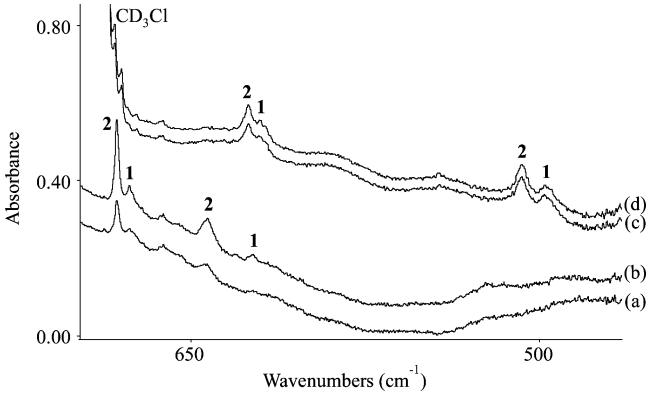

Figure 6. Infrared spectra in the 690−470 cm^{-1} region for laser-ablated Th atoms co-deposited with (a) 0.5% CH_3Cl in excess argon and (b) after full-arc irradiation and for (c) co-deposition of Th atoms with 0.5% CD_3Cl in excess argon and (d) after full-arc irradiation.

is calculated at 539.1 cm^{-1} with 0.3 cm^{-1} ^{13}C and 3.9 cm^{-1} D shifts, and this mode is observed at 518.6 cm^{-1} with 0.3 and 5.3 cm^{-1} isotopic shifts, which shows that this normal coordinate is almost a pure Th−F stretching mode. We note that the ThF_4 antisymmetric Th−F stretching fundamental is at 520 cm^{-1}.[32] The extremely good agreement found between four observed frequencies and the four calculated frequencies with the highest infrared intensities and their isotopic shifts confirms our preparation and identification of the simple actinide methylidene CH_2═ThHF complex.

We have possible evidence for the higher-energy CH_3−ThF isomer. The weak 547.5 and 545.2 cm^{-1} bands and associated 1139.6 and 1136.3 cm^{-1} absorptions also increase upon irradiation, and they can be assigned tentatively to the CH_3−ThF isomer.

CH_3Cl. Reactions of laser-ablated Th atoms and CH_3Cl give three pairs of new absorptions that are illustrated in Figure 5. The strongest diagnostic band at 1401.7 cm^{-1} (labeled **2**) increases upon UV irradiation and is joined by a weaker counterpart at 1426.0 cm^{-1} (labeled **1**). Annealing at 30 K increases **2** at the expense of **1**; subsequent full-arc irradiation reverses this process, and further annealing at 35 K again increases **2** at the expense of **1** (Figure 4d, e, f). Similar behavior is found for the band pairs at 682.0 and 676.6 cm^{-1} and at 643.0 and 623.6 cm^{-1} (labeled **2** and **1**, respectively). We note larger matrix site splittings for the chlorine than the fluorine product: this may be the result of the larger halogen interacting with more argon atoms.

The experiments were repeated with CD_3Cl as the reagent, and the strongest feature at 1401.7 cm^{-1} shifted to 1003.9 cm^{-1} (H/D ratio 1.396), which is again appropriate for a Th−H(D) stretching mode. Figure 6 illustrates the CD_3Cl counterparts of the new lower-frequency bands, which show different deuterium shifts, as listed in Table 3.

The calculated frequencies for CH_2═ThHCl are also listed in Table 3, and the agreement is comparable to that described above for CH_2═ThHF. The strong Th−H stretching mode in this case is calculated 1.9% too high by the B3LYP functional. Again the 2700−2800 cm^{-1} region was checked and found to be free of product absorption. The next strong fundamental is the mostly Th═C stretching mode computed at 685.2 cm^{-1} with a 61.2 cm^{-1} deuterium shift: these

Table 3. Observed and Calculated Fundamental Frequencies of CH_2═ThHCl in the Singlet Ground Electronic State[a]

approximate mode	CH_2═ThHCl		CD_2═ThDCl	
	obsd[b]	calcd (int)	obsd[b]	calcd (int)
CH stretch		3147.8 (2)		2523.1 (2)
CH stretch		2829.1 (11)		2062.0 (3)
Th−H stretch	1426.0, **1401.7**	1428.5 (479)	−[c], **1003.9**	1008.8 (150)
CH_2 scis		1347.6 (21)		1025.7 (116)
Th═C stretch	**682.0**, 676.6	685.2 (137)	**625.2**, 620.2	624.0 (106)
CH_2 wag	**643.0**, 623.6	652.6 (151)	**507.5**, 496.7	509.5 (106)
CThH bend		505.2 (57)		386.3 (37)
CH_2 rock		412.2 (48)		288.5 (21)
HCThH dist		340.2 (108)		314.5 (87)
Th−Cl stretch		294.9 (24)		229.9 (14)
CH_2 twist		232.2 (46)		169.0 (23)
CThCl bend		95.4 (3)		87.5 (10)

[a] Frequencies and intensities are in cm^{-1} and km/mol, respectively. Intensities are all calculated values using B3LYP/6-311++G(3df,3pd)/SDD. [b] Absorption **2** in each observed pair, which increases on photolysis and annealing, is in bold type. Absorption **1** in each observed pair, which increases less on photolysis and decreases on annealing, is in regular type. [c] Masked by CD_3Cl precursor.

predictions are a good match for the **2** bands at 682.0 and 625.2 cm^{-1} (56.8 cm^{-1} redshift). The next strong absorption is the CH_2 wagging mode predicted at 652.6 cm^{-1} with a larger 155.9 cm^{-1} deuterium shift and observed at 643.0 cm^{-1} with a 135.5 cm^{-1} deuterium shift. The discrepancy in deuterium shifts is the result of anharmonicity in the observed wagging absorption not accounted for in the harmonic calculation. In addition, the calculation apparently overestimates the intensity of this mode. Finally, the excellent agreement between the three strongest calculated frequencies for CH_2═ThHCl and the three observed absorptions supports our assignment. Such agreement is expected for the B3LYP functional.[33]

The first product expected in the Th/CH_3Cl reaction is the insertion species CH_3−ThCl, whose triplet ground state (C−Th, 2.413 Å; Th−Cl, 2.600 Å) is 9 kcal/mol higher in energy than singlet CH_2═ThHCl described above. The strongest infrared band for CH_3−ThCl is the Th−Cl stretching mode computed at 302.4 cm^{-1} (64 km/mol), which is below the range of our FTIR instrument.

The B3LYP and CCSD structures for CH_2═ThHCl illustrated in Figures 3 and 4 have essentially the same parameters, which again validates the use of DFT for these

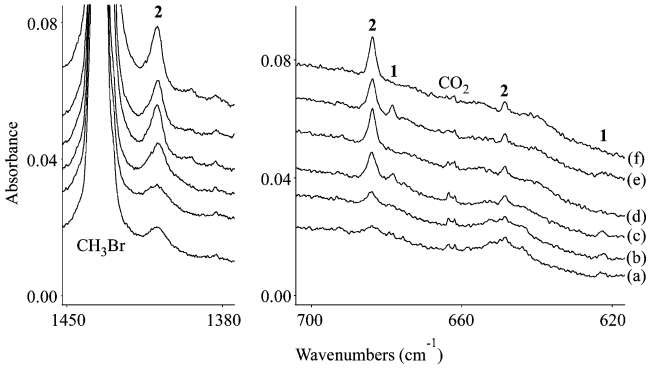

Figure 7. Infrared spectra in the 1450−1380 and 700−620 cm^{-1} regions for laser-ablated Th atoms co-deposited with CH_3Br in excess Ar at 8 K: (a) Th + 0.5% CH_3Br in Ar co-deposited for 1 h, (b) after photolysis with a Pyrex filter, (c) after full-arc photolysis without a filter, (d) after annealing at 30 K, (e) after photolysis without a filter, and (f) after annealing at 35 K.

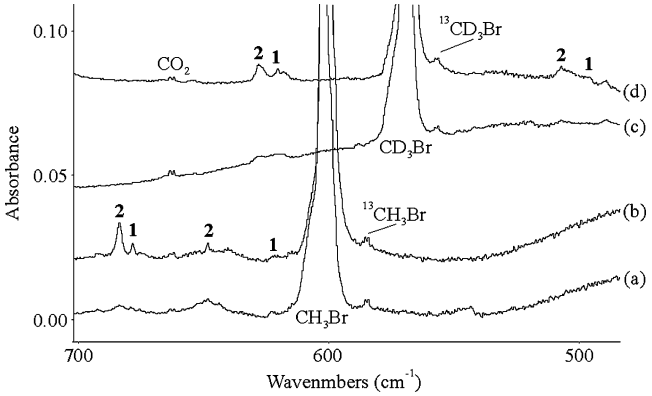

Figure 8. Infrared spectra in the 700−490 cm^{-1} region for laser-ablated Th atoms co-deposited with (a) 0.5% CH_3Br in excess argon and (b) after full-arc irradiation and for (c) co-deposition of Th atoms with 0.5% CD_3Br in excess argon and (d) after full-arc irradiation.

species. Notice also that the agostic angles are slightly smaller, the C═Th bond lengths are slightly longer, and the Th−H bond lengths are slightly shorter than for the F counterpart. Finally, we attempted to calculate the cis-agostic CH_2═ThClH isomer at the B3LYP level, and this structure converged to the more stable trans isomer. However, the Th−H and Th−Cl bonds were exchanged in the trans structure (Figure 3), and a single-point calculation was performed. With zero point-energy correction, this cis structure is 3.6 kcal/mol higher in energy than the converged trans minimum-energy structure.

CH_3Br. Thorium and CH_3Br produce two strong new absorptions at 1409.5 and 684.0 cm^{-1} and a weak 648.6 cm^{-1} band, which are labeled **2** in Figure 7. The **1** matrix-site counterpart expected near 1430 cm^{-1} is covered by CH_3Br, and the lower frequency **1** counterpart appears at 678.4 cm^{-1}. The strong 1409.5 cm^{-1} absorption shifts to 1008.2 cm^{-1} with CD_3Br (H/D ratio 1.398). Figure 8 illustrates the lower region and shows that the 684.0 cm^{-1} band shifts to 628.1 cm^{-1} on CD_3Br substitution, and the weak 648.6 cm^{-1} band shifts to 507.1 cm^{-1} with CD_3Br.

The calculated and observed frequencies for the anticipated CH_2═ThHBr product are compared in Table 4. In this case, the CH_3−ThBr insertion product is 7 kcal/mol higher in energy. The strong Th−H stretching mode is calculated only

Table 4. Observed and Calculated Fundamental Frequencies of CH_2═ThHBr[a]

approximate mode	CH_2ThHBr		CD_2ThDBr	
	obsd[b]	calcd (int)	obsd[b]	calcd (int)
CH stretch		3147.6 (1)		2325.2 (2)
CH stretch		2827.0 (9)		2060.6 (2)
Th−H stretch	**1409.5**	1427.2 (487)	**1008.2**	1008.3 (161)
CH_2 bend		1347.3 (21)		1026.3 (112)
Th═C stretch	**684.0**, 678.4	691.8 (141)	**628.1**, 620.4	629.3 (109)
CH_2 wag	**648.6**, 622.6	655.4 (148)	**507.1**, 495.7	511.9 (104)
CThH bend		504.8 (49)		386.2 (27)
HCThH dist.		402.2 (43)		287.8 (30)
CH_2 twist		338.4 (59)		243.6 (42)
Th−Br stretch		226.2 (76)		199.8 (22)
CThBr bend		197.4 (11)		157.9 (20)
CH_2 rock		91.4 (10)		83.0 (8)

[a] Frequencies and intensities are in cm^{-1} and km/mol, respectively. Intensities are all calculated values using B3LYP/6-311++G(3df,3pd)/SDD. [b] Absorption **2** in each observed pair, which increases on photolysis and annealing, is in bold type. Absorption **1** in each observed pair, which increases less on photolysis and decreases on annealing, is in regular type.

Table 5. Natural Charge and Electron Configuration Calculated for the CH_2═ThHX (X = F, Cl, Br) Species Using the B3LYP Density Functional

species	atom	q[a]	s	p	d	f
CH_2═ThHF	F[b]	−0.81	1.98	5.82	0.01	
	Th[c]	2.77	0.25	0.03	0.72	0.29
	C[d]	−1.64	1.41	4.19/0.01	0.03	
	H[e]	−0.68	1.67	0.01		
	H[f]	0.17	0.83			
	H[g]	0.20	0.80			
CH_2═ThHCl	Cl[h]	−0.73	1.97	5.74	0.02	
	Th[c]	2.68	0.27	0.03	0.77	0.29
	C[d]	−1.64	1.41	4.19/0.01	0.03	
	H[e]	−0.67	1.66	0.02		
	H[f]	0.16	0.83			
	H[g]	0.20	0.79			
CH_2═ThHBr	Br[i]	−0.71	1.98	5.72	0.02	
	Th[c]	2.66	0.28	0.03	0.79	0.28
	C[d]	−1.65	1.42	4.19/0.01	0.03	
	H[e]	−0.67	1.66	0.02		
	H[f]	0.16	0.83			
	H[g]	0.21	0.79			

[a] Natural charge. [b] 2s, 2p, 3d. [c] 7s, 7p, 6d, 5f. [d] 2s, 2p/3p, 3d. [e] Hydrogen bonded to thorium: 1s, 2p. [f] Hydrogen bonded to carbon, closest to thorium: 1s. [g] Hydrogen bonded to carbon, furthest from thorium: 1s. [h] 3s, 3p, 3d. [i] 4s, 4p, 4d.

1.2% too high for CH_2═ThHBr. The next strongest infrared absorption is the mostly C═Th stretching mode predicted at 691.8 cm^{-1} with a 62.5 cm^{-1} CD_3Br shift. The 684.0 cm^{-1} band exhibits a CD_3Br shift of 55.9 cm^{-1}, which is in agreement with the prediction considering anharmonicity. The CH_2 wag is computed at 655.4 cm^{-1} with 143.5 cm^{-1} deuterium shift, and the 648.6 cm^{-1} band with 141.5 cm^{-1} deuterium shift is appropriate for this mode. The overall agreement between observed and calculated frequencies supports our identification of CH_2═ThHBr. Taken as a family group, the observed spectra and calculated frequencies fit together nicely and support our preparation of the three thorium methylidenes CH_2═ThHX for X=F, Cl, and Br. Additional computed properties of these molecules are compared in Table 5. The dipole moments are 5.07, 5.05, and 5.00 D, respectively. Finally, reactions to form the three thorium methylidene hydride halide complexes are all exothermic (B3LYP).

$$Th + CH_3F \rightarrow CH_2{=}ThHF \quad (\Delta E = -130 \text{ kcal/mol}) \quad (1a)$$

$$Th + CH_3Cl \rightarrow CH_2{=}ThHCl \quad (\Delta E = -120 \text{ kcal/mol}) \quad (1b)$$

$$Th + CH_3Br \rightarrow CH_2{=}ThHBr \quad (\Delta E = -119 \text{ kcal/mol}) \quad (1c)$$

The structure calculations for $CH_2{=}ThHBr$ follow the same trends described above for $CH_2{=}ThHCl$, which is analogous to that found for the $CH_2{=}TiHX$ methylidene complexes,[1,4] namely a slight increase in the agostic bonding interaction with the heavier halogen substituent on the basis of C=Th bond lengths and agostic H−C−Th bond angles. In contrast to the F and Cl cases, the cis-agostic $CH_2{=}ThBrH$ isomer converged to a stable minimum with a slightly longer C=Th bond (2.124 Å), a larger agostic angle (105.6°), and all real frequencies. This cis-agostic structure is 1.4 kcal/mol higher in energy than the trans-agostic form shown in Figure 3. The three observable frequencies are calculated as 1412.6 (518), 658.6 (186), and 654.0 cm^{-1} (118 km/mol) for the cis-agostic isomer. Since we expect the B3LYP functional to predict frequencies higher than observed,[33] the longer C=Th bond and lower frequency for the cis-form are not in agreement with experiment. Hence, we have trapped the more stable trans-agostic $CH_2{=}ThHBr$ isomer.

Family Trends and Agostic Bonding. The agostic structure of $CH_2{=}ThHF$ is comparable to that in the related Group 4 methylidene complexes. The CH_2Th subunit is almost coplanar, but the H and F atoms on Th are out of this plane. The agostic distortion of the CH_2 group to place one H much closer to Th than the other results in an agostic H−C−Th angle of 94.7° and helps to stabilize the C=Th double bond (2.129 Å). This is more agostic distortion than calculated for the analogous $CH_2{=}HfHF$ molecule, particularly when the longer C−Th bond length is considered, which represents a reversal in the Group 4 trend, as summarized in Table 2. We note that the Mulliken charge (1.88) computed on Th is substantially larger than that for Hf (1.21) and suggest that this charge, the more electropositive nature of Th, and the larger atomic radius enhance the agostic interaction. The natural valence-electron configuration calculated for Th is dominated by 6d in the $CH_2{=}ThHF$ molecule (Table 5). Furthermore, the structures and spectra of the Group 4 $CH_2{=}MHF$ methylidenes are similar,[1−4] and thorium is behaving much like a heavier Group 4 transition metal in this actinide methylidene complex; however, the larger atomic size resulting from shell expansion gives this actinide different chemical properties. Finally, the unsubstituted $CH_2{=}ThH_2$ methylidene dihydride has similar matrix infrared spectra and comparable calculated structural features (agostic H−C−Th angle 95.6°, C=Th bond length 2.116 Å).[24]

The structure calculated for $CH_2{=}ThHCl$ is changed slightly from that for $CH_2{=}ThHF$ (Figure 3). The C=Th bond is 0.015 Å shorter; the agostic H−C−Th angle is 1.9° smaller, and the Th−H bond is 0.015 Å shorter. These small decreases in bond length are associated with slightly higher observed C=Th and Th−H stretching frequencies (compare Tables 1 and 3). These changes continue but are even smaller for $CH_2{=}ThHBr$ compared to $CH_2{=}ThHCl$, and the increased agostic interaction in $CH_2{=}ThHBr$ and $CH_2{=}ThHCl$ relative to $CH_2{=}ThHF$ cannot be attributed to increased charge on the Th center (natural charge decreases, Table 5).

Finally, we note that the $CH_2{=}ThHX$ α−H transfer complexes are all more stable (5, 9, and 7 kcal/mol, respectively) than their presumed CH_3-ThX precursors. This differs from the Group 4 case where the insertion products are more stable.[1−4] A salient difference in the organometallic chemistry is the prevalence of Group 4 methylidene complexes and the dearth of thorium counterparts.[20,21] We can only speculate that, because of shell expansion and the larger metal size, the thorium complexes are more reactive and proceed to even more stable products in a synthetic chemical system. Here, the thorium methylidene complexes are blocked from further reaction by the argon matrix cage.

Conclusions

Laser-ablated Th atoms react with methyl halides to form the actinide methylidenes, $CH_2{=}ThHX$ (X = F, Cl, Br), as the major products which are trapped in solid argon. These molecules are identified through the effect of isotopic substitution on the infrared spectra and comparison to frequencies and isotopic shifts computed by density functional theory. The Th−H stretching, C=Th stretching, and CH_2 wagging frequencies in these molecules increase slightly on going from X = F to Cl to Br. The B3LYP computed structure for $CH_2{=}ThHF$ shows evidence of agostic distortion comparable to that computed for $CH_2{=}ZrHF$, although the C=Th bond is longer than the C=Zr bond. The $CH_2{=}ThHX$ trans-agostic structure is more stable. In addition, less stable cis-agostic structures for X = F and Cl converge to the more stable trans-agostic forms, and for X = Br, a 1.4 kcal/mol higher energy cis form converges to a stable minimum. Finally, structures computed at the more rigorous CCSD level of theory for these $CH_2{=}ThHX$ complexes are virtually the same as those calculated at the DFT level, which substantiates this application of DFT and shows that the B3LYP density functional provides a very good description of structure and related vibrational frequencies for these actinide methylidene complexes.

Acknowledgment. We gratefully acknowledge financial support for this research under NSF Grant CHE 03-52487 and fellowship support (J.T.L.) from the NSF IGERT Grant 99-72790. This research was performed in part using the Molecular Science Computing Facility (MSCF) in the William R. Wiley Environmental Molecular Sciences Laboratory, a national scientific user facility sponsored by the U.S. Department of Energy's Office of Biological and Environmental Research and located at the Pacific Northwest National Laboratory. Pacific Northwest is operated for the Department of Energy by Battelle.

IC051153W